DOI: 10.1002/cphc.201100583

Combination of MOFs and Zeolites for Mixed-Matrix Membranes

Beatriz Zornoza,[a] Beatriz Seoane,[a] Juan M. Zamaro,[b] Carlos Téllez,[a] and Joaquín Coronas*[a]

Mixed-matrix membranes (MMMs) were prepared by combinations of two different kinds of porous fillers [metal-organic frameworks (MOFs) HKUST-1 and ZIF-8, and zeolite silicalite-1] and polysulfone. In the search for filler synergy, the MMMs were applied to the separation of CO_2/N_2, CO_2/CH_4, O_2/N_2, and H_2/CH_4 mixtures and we found important selectivity improvements with the HKUST-1-silicalite-1 system (CO_2/CH_4 and CO_2/N_2 separation factors of 22.4 and 38.0 with CO_2 permeabilities of 8.9 and 8.4 Barrer, respectively).

1. Introduction

Mixed-matrix membranes (MMMs) are produced by the incorporation of inorganic or hybrid fillers, such as zeolites,[1,2] ordered mesoporous silica,[3–5] non-porous silica,[6,7] carbon molecular sieves,[8] carbon nanotubes,[9,10] and metal-organic frameworks (MOFs)[11,12] into polymeric membrane materials. These hybrid films have the advantage of combining the benefits of both phases: the superior gas transport properties of molecular sieves with the desirable mechanical properties, low price and good processability of polymers.[1,13]

Zeolites are one of the most versatile nanoporous fillers when considering aspects such as chemical composition, particle size, shape, and textural properties. However, from the point of view of compatibility between the polymer phase and the filler, MOFs have an evident advantage over zeolites. In fact, besides sharing the crystallinity and textural properties common to zeolites,[14,15] MOFs are highly versatile materials in the sense that by choosing the appropriate organic ligand it is possible to determine the size, shape and chemical functionality of their cavities.[16–19] MOFs have a great potential for application in gas storage,[15] drug delivery,[20] gas separation with membranes,[12] enantioselective separations,[21] sensors,[22] and heterogeneous catalysis.[23]

MMMs containing MOFs, such as CuTPA/Poly(vinyl acetate),[24] Cu-4,4′-bypiridine-hexafluorosilicate (Cu-BPY-HFS)/polyimide,[11] MOF-5/polyimide,[25] $Cu_3(BTC)_2$/polyimide,[26,27] ZIF-8/1,4-phenylene ether-ether-sulfone,[28] ZIF-8/polyimide,[29] and ZIF-90/polyimide,[12] have been obtained. These membranes have shown good separation performance of binary mixtures, such as CO_2/CH_4, H_2/CO_2, and CH_4/N_2. Even though a considerable research effort has been made on the use of nanoporous fillers in MMMs, the suggested combination of zeolite and MOF in the same MMM has not been reported to date. Therefore, the aim herein is the development of MOF-silicalite-1-polysulfone MMMs. For some of the gas mixtures studied, these MMMs are able to produce a synergetic enhancement in terms of selective gas transport when compared either to the pure polymer or to MMMs with only one filler type.

2. Results and Discussion

2.1. Membrane Preparation and Characterization

The requirements of a porous filler to make up a MMM include porosity and textural properties but also good dispersibility and chemical affinity with the polymer to avoid aggregation and particle-surrounding areas with poor interaction.[30] By using fillers of a different nature in the same MMM, synergy effects may appear, leading to membranes with better permeation properties than those of MMMs with only one filler type. Hence, the working hypothesis is that filler particles of the same nature may agglomerate and then lead to bad dispersion. In contrast, two different types of particles may lead to a complementary interaction, improving filler dispersion. In addition, the presence of the two kinds of porous fillers may add an extra stability to the casting dispersion, in agreement with the findings that are shown herein as well.

Silicalite-1 (labeled S1C), with 442($\pm$1) $m^2 g^{-1}$ of BET area and 0.55 nm pore size, is probably the most extensively studied microporous filler for MMMs. Due to its hydrophobicity,[31] silicalite-1 presents good interaction with most gas permeation polymers.[32] This interaction can be improved through controlled deposition of $Mg(OH)_2$ nanostructures.[33,34] ZIF-8 and HKUST-1 have cages with similar diameters (about 1.1 nm) but different window sizes: 0.34 nm for ZIF-8[35] and 0.6 nm for HKUST-1.[36] Similar values of BET area were measured for ZIF-8 [1924($\pm$17) $m^2 g^{-1}$] and HKUST-1 (1925($\pm$37) $m^2 g^{-1}$). Due to the

[a] B. Zornoza,[+] B. Seoane,[+] Dr. C. Téllez, Prof. Dr. J. Coronas
Chemical and Environmental Engineering Department
and Instituto de Nanociencia de Aragón
Universidad de Zaragoza, 50018 Zaragoza (Spain)
E-mail: coronas@unizar.es

[b] Dr. J. M. Zamaro
Instituto de Investigaciones en Catálisis y Petroquímica
INCAPE (FIQ, UNL, CONICET)
Santiago del Estero 2829, 3000 Santa Fe (Argentina)

[+] These two authors contributed equally to this work.

Supporting information for this article is available on the WWW under http://dx.doi.org/10.1002/cphc.201100583.

partially organic nature of MOFs, their interaction with the polymer must also be favored.

Figures 1a and b correspond to SEM cross sections of ZIF-8- and HKUST-1-PSF MMMs. The appearance in both cases is of homogeneous dispersion and intimate filler-polymer interaction. Similar features are observed in Figures 1c and d corresponding to the combination of fillers: ZIF-8/S1C-PSF and HKUST-1/S1C-PSF MMMs, where the coexistence of both silicalite-1 and MOF fillers is evident. The TEM insets emphasize on the good filler-polymer interaction even though SEM images, because of the sample preparation methodology, may suggest defective zeolite- or MOF-polymer interfaces.

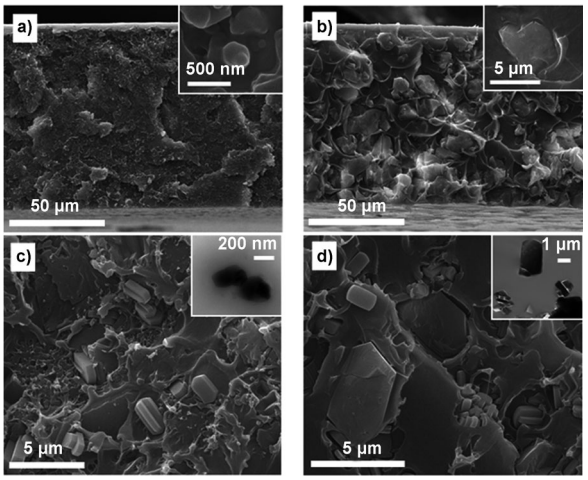

Figure 1. Cross-section SEM images of MMMs: a) 16 wt% ZIF-8-PSF (the inset shows a ZIF-8 particle surrounded by polymer); b) 16 wt% HKUST-1-PSF (the inset shows a HKUST-1 particle); c) 8 wt% ZIF-8 + 8 wt% S1C-PSF (with TEM inset showing a ZIF-8 particle); d) 8 wt% HKUST-1 + 8 wt% S1C-PSF (with TEM inset showing a silicalite-1 particle).

In the XRD patterns in Figure 2 it can be seen that most of the main MOFs and silicalite-1 reflection peaks are present in the composite membranes. This also evidences that the membrane preparation procedure did not alter the filler crystallinities. In addition, the broad peak for the pure polymer centered at $2\theta = 17.3^\circ$ (d-spacing = 5.1 Å) moves to about $2\theta = 17.9$–18.2° (d-spacing = 4.9 Å), consistent with strong interaction between continuous and disperse phases, which would reduce the distance between polymer chains.[37] Additionally, the main peaks of the MOFs (at $2\theta = 7.2^\circ$ for ZIF-8, and 11.4° for HKUST-1) displace to higher angles, suggesting some deformation in their crystal lattices which could be attributed to the interaction with the polymer. Such displacements are not evident for silicalite-1 filler.

When FTIR analyses were conducted on the samples (see Figures S1 and S2 in the Supporting Information), weak displacements were observed mainly in the 1235 cm^{-1} band, corresponding to the Ar–O–Ar stretching (Ar being the aryl group) in the polysulfone matrix.[32,38] These bands are displaced toward higher wavenumbers due to a strengthening in these bonds, accounting for the filler–polymer interactions described above. The displacements are more marked for ZIF-8-containing samples.

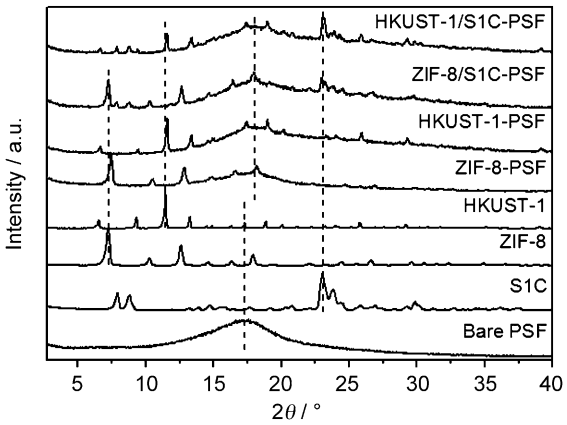

Figure 2. XRD patterns of (from bottom to top): pure PSF, silicalite-1 (S1C), ZIF-8, HKUST-1, 16 wt% ZIF-8-PSF MMM, 16 wt% HKUST-1-PSF MMM, 8 wt% ZIF-8 + 8 wt% S1C-PSF MMM, and 8 wt% HKUST-1 + 8 wt% S1C-PSF MMM.

Even though no specific differences were found by XRD and FTIR for the combined MMMs, when they were prepared (with the same 16 wt% total loading) with silicalite-1 and HKUST-1 there was an increase in T_g (glass transition temperature) from 188.5 °C for pure PSF to 194.2 °C for S1C-PSF, 193.8 for HKUST-1-PSF, and 195.0 °C for HKUST-1/S1C-PSF. The combination of both HKUST-1 and S1C fillers may produce an increasing rigidity and restricted motion of the polymer, due to the chemical interactions established between the chain polymer and external surface areas, higher than those observed for the two separated fillers. This suggests a subtle synergy effect between both fillers. The synergy may arise from the different surface chemistry of both types of fillers, which helps the dispersion and disaggregation in the polymer matrix. Two filler particles with the same structure and chemistry would have a higher tendency to agglomerate than two particles different in nature. The increases in T_g for MMMs containing ZIF-8 (with the same 16 wt% total loading) were less pronounced than those for MMMs containing HKUST-1: 193.7 °C for ZIF-8-PSF, and 194.4 °C for ZIF-8/S1C-PSF. Finally, analogous T_g variations from 188.5 to 196.0 °C have been reported for 0–16 wt% mesoporous silica-PSF MMMs.[38]

In agreement with these results, the TGA analyses of the different membranes (Figure S3, Supporting Information) and the corresponding derivatives (Figure S4, Supporting Information) reveal marked differences for the HKUST-1-containing samples. The second minimum of the polymer degradation is at an intermediate temperature for the HKUST-1/S1C-PSF MMM (~610 °C) when compared with the S1C-PSF (~650 °C) and HKUST-1-PSF (~595 °C) MMMs, even though the first minimum was at the same approximate temperature for the two membranes with HKUST-1. For comparison, Figure S5 (Supporting Information) shows TGA curves of pure fillers.

Additional characterization arises when the contact angle (CA) is measured on the different membranes. Even though silicalite-1 is a hydrophobic zeolite,[31,39] S1C-PSF is less hydrophobic ($71.9 \pm 0.4^\circ$) than pure PSF ($75.4 \pm 0.7^\circ$), which can be due

to the presence of surface silanol groups.[40] Besides, because HKUST-1 is hydrophilic,[36,41] HKUST-1-PSF (63.3 ± 1.4°) is a less hydrophobic membrane. Interestingly, HKUST-1/S1C-PSF (67.4 ± 1.4°) MMM gives rise to an intermediate CA, which can be attributed to the better particle dispersion achieved by the combination of fillers. The ZIF-8 hydrophobicity[41] is efficiently expressed in ZIF-8-PSF (77.6 ± 0.4°) and ZIF-8/S1C-PSF (74.1 ± 0.8°) MMMs. An analogous CA (75°) has been reported for pure PSF.[42,43]

2.2. Gas Separation

The advantage of filler combinations is clearly demonstrated from the point of view of gas separation performance in relevant CO_2/CH_4 (natural gas upgrading), CO_2/N_2 (CO_2 capture), O_2/N_2 (air separation), and H_2/CH_4 (H_2 purification) mixtures. As shown in Figure 3, all the fillers, at the same total loading of 16 wt%, increase the CO_2 permeability when compared to that of the bare polymer in any of the two CO_2-containing mixtures. The disruption of polymer chain packing and linking due to the presence of fillers, as mentioned above, which leads to an increase in polymer matrix free volume, explains this permeability improvement in part.

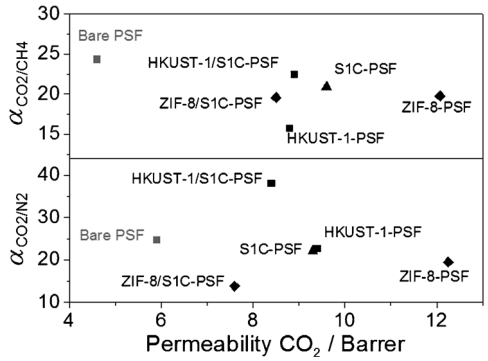

Figure 3. CO_2/CH_4 (top) and CO_2/N_2 (bottom) separation selectivities as a function of CO_2 permeability for the different MMMs prepared (Figures 1 and 2).

In addition, the CO_2 adsorption capacity (Figure 4) is considerably higher for HKUST-1 than for the other two fillers. However, the maximum separation selectivities for both mixtures ($\alpha_{CO2/CH4} = 22.4$ with 8.9 Barrer for CO_2, and $\alpha_{CO2/N2} = 38.0$ with 8.4 Barrer for CO_2) were only achieved when HKUST-1 was combined with silicalite-1 (HKUST-1/S1C-PSF MMM). The combination of ZIF-8 and silicalite-1 (ZIF-8/S1C-PSF MMM) did not improve the separation results for either S1C-PSF or ZIF-8-PSF MMMs. In this case, the relatively large silicalite-1 crystals could not be intercalated between small ZIF-8 particles (ca. 100 nm) that also have a lower affinity towards CO_2 (Figure 4). Finally, ZIF-8 alone produced the highest increase of CO_2 permeability, which can be attributed not only to its textural properties but also to its small particle size, giving rise to the formation of poorly dispersed aggregates.

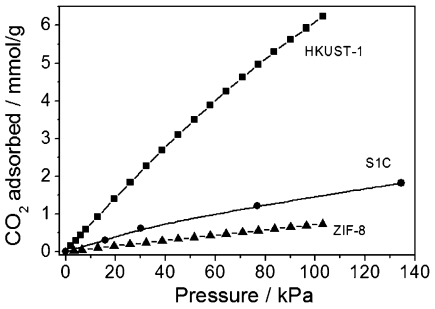

Figure 4. CO_2 adsorption isotherms of ZIF-8 and HKUST-1 at 25 °C, and silicalite-1 (S1C) at 35 °C. For S1C the data is taken from a previous publication.[32]

When the same membranes described above were applied to the O_2/N_2 and H_2/CH_4 separations (Figure 5), mixtures in which the separation mechanism is based mainly on diffusion and not on adsorption differences,[32] the combination of HKUST-1 and silicalite-1 gave rise to important selectivity achievements. This is probably due to an improved molecular diffusion mechanism through zeolite crystals provided by their synergy with HKUST-1. However, the ZIF-8-PSF MMM produced the best selectivity-permeability results (Figure 5, $\alpha_{O2/N2} = 8.3$ with 2.6 Barrer for O_2, and $\alpha_{H2/CH4} = 118$ with 39.8 Barrer for H_2) due to an increase in free volume (as suggested for ZIF-8-polyimide MMMs)[29] together with an efficient molecular separation effect (based on diffusion differences) because of the small pore aperture of ZIF-8 (0.34 nm) compared to those of HKUST-1 (0.6 nm) and silicalite-1 (0.55 nm). It is worth mentioning that the separation selectivities were obtained from the testing of mixtures and not from single gas permeabilities.

Finally, using the models of Moore and Koros[44] together with a volume faction of 0.20 from the weight filler loading and PSF (1.24 g cm^{-3}) and ZIF-8 (0.95 g cm^{-3})[35] densities and using CO_2, CH_4, H_2, O_2 and N_2 permeabilities reported for a pure ZIF-8 membrane,[45] defective voids of about 3.1 nm were estimated from our CO_2/CH_4 separation results, while no defects appeared in the calculations based on O_2/N_2 and H_2/CH_4

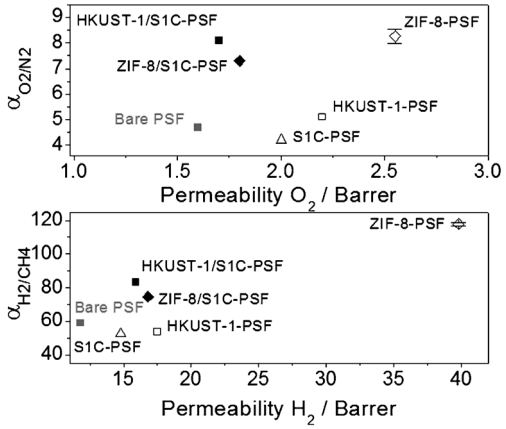

Figure 5. O_2/N_2 (top) and H_2/CH_4 (bottom) separation selectivities as a function of O_2 and H_2 permeabilities for the different MMMs prepared (Figures 1 and 2).

results. These estimations indicate that defective voids would affect the ZIF-8-containing membrane performance only in adsorption-based separations. In consequence, the good performance of HKUST-1/S1C MMMs in adsorption-based separations would be in line with low-defective membranes.

3. Conclusions

Using fillers of different natures in the same MMM may produce synergy effects leading to membranes with better permeation properties than those corresponding to MMMs with only one filler type. The different surface chemistry of both types of fillers may help the dispersion and disaggregation inside the polymer matrix. In particular, because of the high CO_2 adsorption of HKUST-1, the combination of HKUST-1 and silicalite-1 leads to the best separation performance in CO_2-containing mixtures. On the other hand, ZIF-8-containing MMMs give rise to the best performance when mixtures are separated based on diffusion differences between permeating molecules.

The results achieved herein clearly point towards a new research scenario in which not only MOF–zeolite but also MOF–MOF, zeolite–zeolite and other combinations, including ordered mesoporous materials and non-permeable fillers like dense silica, could be examined in the search for improvements in gas separation using MMMs. In addition, the study of high-permeability polymers[12,33,46] would complete the picture of performance enhancement that may be achieved with this new approach.

Experimental Section

HKUST-1 and ZIF-8 (Basolite C 300 and Basolite Z1200, respectively) were purchased from Sigma–Aldrich. HKUST-1 has a mean particle size of 16 μm while for ZIF-8 the mean size is 4.9 μm. However, SEM observation reveals particle size ranges of 7.7 (±2.7) μm for HKUST-1 and of about 113 (±32) nm for ZIF-8. Silicalite-1 crystals (labeled S1C) with dimensions of around 0.3 μm × 1 μm × 2.0 μm were prepared according to a procedure described in a previous work.[32]

Polysulfone (PSF) Udel P-3500 (kindly supplied by Solvay Advanced Polymers) was used as the continuous phase for the MMMs. Before fabricating the membranes, PSF was dried under vacuum conditions at 120 °C for 24 h. First, bare PSF membranes were prepared by dissolving the polymer (0.4 g) in chloroform (3.6 g, Sigma–Aldrich) and stirring overnight. The preparation of the zeolite and/or MOF MMMs (S1C-PSF, ZIF-8-PSF, HKUST-1-PSF, and their filler mixtures at 50 wt%, ZIF-8/S1C-PSF and HKUST-1/S1C-PSF) required an additional step for dispersing the fillers in the solvent in an ultrasonic bath for 15 min. For MMMs the percentage of the solvent was identical (proportion of 90/10 wt% solvent/fillers-polymer mixture, allowing good viscosity of the casting solution). PSF was then added and the whole mixture was stirred overnight finishing with three intervals of sonication to guarantee a well-dispersed solution. Subsequently, the membranes were cast on flat glass plates, and left partially closed to slow down the natural evaporation of solvent at room temperature. Once dried, the membranes were placed in a Memmert VO 200 vacuum oven at 120 °C for 24 h to remove the remaining solvent. The membranes obtained (with 16 wt% total loadings of pure or mixed filler) had a thickness of 90(±8) μm, measured using a micrometer (accuracy of ±0.001 mm, Mitutoyo Corp.).

X-ray diffraction (XRD) of the MMMs were performed at ambient temperature on a rotating anode diffractometer (D-Max Rigaku) using monochromatic CuK_α radiation with $\lambda = 1.5418$ Å at a scanning rate of 0.03° s^{-1} between $2\theta = 2.5°$ and 40°. Scanning electron microscopy (SEM) images were collected with a JEOL JSM 6400 instrument (Jeol Corp.) operating at 20 kV. With this aim, sectional pieces of the membrane were prepared by freeze fracturing after immersion in liquid N_2. For TEM analysis (transmission electron microscopy JEOL 2000 FXII, Jeol Corp.), samples were embedded in an epoxy cold-setting embedding resin (Epofix, Electron Microscopy Sciences): 15 parts of resin and 2 parts of hardener were mixed. The curing time was 8 h at room temperature and the cross section pieces were sliced into 30–60 nm thick sections using a RMC MT-XL ultramicrotome with a Standard Ultraknife 45°, with a 3 mm diamond blade (Drukker). The thin slices were placed on carbon–copper grids and observed at 200 kV.

Thermogravimetric analyses (TGA) were performed under air flow from 25 to 800 °C with a heating rate of 10 °C min^{-1} using a Mettler Toledo TGA/SDTA851[e] system. Differential scanning calorimetry (DSC) measurements were taken using Mettler Toledo DSC822[e] equipment to estimate the glass transition temperature (T_g) of the MMMs. Samples were scanned up to 250 °C with a heating rate of 20 °C min^{-1}. Two consecutive runs were performed and T_g was calculated from the middle point of the slope transition in the DSC curve.

To measure the contact angle (CA), deionized water was dropped (5 μL) onto the top surface of bare PSF and the different MMMs with a micro-syringe. Five measurements at different locations were made and the average was used to represent the CA value for the membranes examined.

Attenuated total internal reflection Fourier-transform infrared (ATR-FTIR) spectroscopy of the membranes was performed using a Bruker Vertex 70 FTIR spectrometer equipped with a DTGS detector and a Golden Gate diamond ATR accessory. Spectra were recorded by averaging 40 scans in the 4000–600 cm^{-1} wavenumber range at a resolution of 4 cm^{-1}. Data were registered with OPUS software from Bruker Optics.

Ar and CO_2 isotherms and BET specific surface areas of the powder materials were obtained at −186 °C and 25 °C, respectively, after outgassing at 200 °C for 10 h. For these measurements, TriStar 3000 and ASAP 2020, both from Micromeritics, were used.

A detailed description of the gas permeation setup is reported elsewhere.[38] The membranes with an area of 15.2 cm^2 were placed inside a permeability module composed of two stainless steel parts with a cavity to locate the membrane and a macroporous disk support (20 μm nominal pore size, Mott Co.) gripped inside with Viton o-rings. Mass flow meter controllers (Alicat Scientific) were used for feed and sweep gas provision to the membrane module. CO_2/N_2, CO_2/CH_4 and O_2/N_2 [25/25 cm^3(STP) min^{-1}] separate mixture streams were fed at 275 kPa to the retentate side, while the permeate side was swept with 5 cm^3(STP) min^{-1} mass-flow controlled stream of He at atmospheric pressure. For H_2/CH_4 separation 1 cm^3(STP) min^{-1} of Ar was used as the sweep gas. Gas concentrations in the outgoing stream were analyzed by an on-line gas micro-chromatograph Agilent 3000 A equipped with TCD. Permeability results, in Barrer (1×10^{-10} cm^3(STP) cm/(cm^2 s cmHg), were obtained once the exit stream of the membrane was stabilized. The real separation selectivity of the mixtures was calculated

as the ratio of experimental permeabilities. All the permeation measurements were performed at 35 °C, controlled by a Memmert UNE 200 oven.

Acknowledgements

Financial support (CIT-420000-2009-32, MAT2010-15870) and FPU Program fellowships (B. Zornoza and B. Seoane) from the Spanish Science and Innovation Ministry are gratefully acknowledged. J. M. Zamaro acknowledges CONICET of Argentina for a grant for a research stay in Spain.

Keywords: gas separation · membranes · metal–organic frameworks · organic–inorganic hybrid composites · zeolites

[1] C. M. Zimmerman, A. Singh, W. J. Koros, *J. Membr. Sci.* **1997**, *137*, 145 – 154.
[2] P. Gorgojo, S. Uriel, C. Téllez, J. Coronas, *Microporous Mesoporous Mater.* **2008**, *115*, 85 – 92.
[3] B. D. Reid, A. Ruiz-Trevino, I. H. Musselman, K. J. Balkus, J. P. Ferraris, *Chem. Mater.* **2001**, *13*, 2366 – 2373.
[4] S. Kim, E. Marand, J. Ida, V. V. Guliants, *Chem. Mater.* **2006**, *18*, 1149 – 1155.
[5] S. Kim, E. Marand, *Microporous Mesoporous Mater.* **2008**, *114*, 129 – 136.
[6] T. C. Merkel, B. D. Freeman, R. J. Spontak, Z. He, I. Pinnau, P. Meakin, A. J. Hill, *Science* **2002**, *296*, 519 – 522.
[7] J. Ahn, W.-J. Chung, I. Pinnau, M. D. Guiver, *J. Membr. Sci.* **2008**, *314*, 123 – 133.
[8] D. Q. Vu, W. J. Koros, S. J. Miller, *J. Membr. Sci.* **2003**, *211*, 335 – 348.
[9] H. L. Cong, J. M. Zhang, M. Radosz, Y. Q. Shen, *J. Membr. Sci.* **2007**, *294*, 178 – 185.
[10] S. Kim, L. Chen, J. K. Johnson, E. Marand, *J. Membr. Sci.* **2007**, *294*, 147 – 158.
[11] Y. F. Zhang, I. H. Musselman, J. P. Ferraris, K. J. Balkus, *J. Membr. Sci.* **2008**, *313*, 170 – 181.
[12] T. H. Bae, J. S. Lee, W. L. Qiu, W. J. Koros, C. W. Jones, S. Nair, *Angew. Chem.* **2010**, *122*, 10059 – 10062; *Angew. Chem. Int. Ed.* **2010**, *49*, 9863 – 9866.
[13] T. S. Chung, L. Y. Jiang, Y. Li, S. Kulprathipanja, *Prog. Polym. Sci.* **2007**, *32*, 483 – 507.
[14] O. M. Yaghi, M. O'Keeffe, N. W. Ockwig, H. K. Chae, M. Eddaoudi, J. Kim, *Nature* **2003**, *423*, 705 – 714.
[15] G. Férey, *Chem. Soc. Rev.* **2008**, *37*, 191 – 214.
[16] M. Eddaoudi, J. Kim, N. Rosi, D. Vodak, J. Wachter, M. O'Keeffe, O. M. Yaghi, *Science* **2002**, *295*, 469 – 472.
[17] S. Kitagawa, R. Kitaura, S. Noro, *Angew. Chem.* **2004**, *116*, 2388 – 2430; *Angew. Chem. Int. Ed.* **2004**, *43*, 2334 – 2375.
[18] H. K. Chae, D. Y. Siberio-Perez, J. Kim, Y. Go, M. Eddaoudi, A. J. Matzger, M. O'Keeffe, O. M. Yaghi, *Nature* **2004**, *427*, 523 – 527.
[19] S. L. Qiu, G. S. Zhu, *Coord. Chem. Rev.* **2009**, *253*, 2891 – 2911.
[20] P. Horcajada, C. Serre, M. Vallet-Regi, M. Sebban, F. Taulelle, G. Ferey, *Angew. Chem.* **2006**, *118*, 6120 – 6124; *Angew. Chem. Int. Ed.* **2006**, *45*, 5974 – 5978.
[21] J. S. Seo, D. Whang, H. Lee, S. I. Jun, J. Oh, Y. J. Jeon, K. Kim, *Nature* **2000**, *404*, 982 – 986.
[22] Y. Takashima, V. M. Martinez, S. Furukawa, M. Kondo, S. Shimomura, H. Uehara, M. Nakahama, K. Sugimoto, S. Kitagawa, *Nat. Commun.* **2011**, *2*, 1 – 8.
[23] S. Naito, T. Tanibe, E. Saito, T. Miyao, W. Mori, *Chem. Lett.* **2001**, 1178 – 1179.
[24] R. Adams, C. Carson, J. Ward, R. Tannenbaum, W. Koros, *Microporous Mesoporous Mater.* **2010**, *131*, 13 – 20.
[25] E. V. Perez, K. J. Balkus, J. P. Ferraris, I. H. Musselman, *J. Membr. Sci.* **2009**, *328*, 165 – 173.
[26] S. Basu, A. Cano-Odena, I. F. J. Vankelecom, *J. Membr. Sci.* **2010**, *362*, 478 – 487.
[27] J. Hu, H. P. Cai, H. Q. Ren, Y. M. Wei, Z. L. Xu, H. L. Liu, Y. Hu, *Ind. Eng. Chem. Res.* **2010**, *49*, 12605 – 12612.
[28] K. Díaz, L. Garrido, M. Lopez-Gonzalez, L. F. del Castillo, E. Riande, *Macromolecules* **2010**, *43*, 316 – 325.
[29] M. J. C. Ordoñez, K. J. Balkus, J. P. Ferraris, I. H. Musselman, *J. Membr. Sci.* **2010**, *361*, 28 – 37.
[30] B. Zornoza, P. Gorgojo, C. Casado, C. Téllez J. Coronas, *Desalination Water Treat.* **2011**, *27*, 42 – 47.
[31] E. M. Flanigen, J. M. Bennett, R. W. Grose, J. P. Cohen, R. L. Patton, R. M. Kirchner, J. V. Smith, *Nature* **1978**, *271*, 512 – 516.
[32] B. Zornoza, O. Esekhile, W. J. Koros, C. Tellez, J. Coronas, *Sep. Purif. Technol.* **2011**, *77*, 137 – 145.
[33] T. H. Bae, J. Q. Liu, J. S. Lee, W. J. Koros, C. W. Jones, S. Nair, *J. Am. Chem. Soc.* **2009**, *131*, 14662 – 14663.
[34] T. H. Bae, J. Q. Liu, J. A. Thompson, W. J. Koros, C. W. Jones, S. Nair, *Microporous Mesoporous Mater.* **2010**, *139*, 120 – 129.
[35] K. S. Park, Z. Ni, A. P. Cote, J. Y. Choi, R. D. Huang, F. J. Uribe-Romo, H. K. Chae, M. O'Keeffe, O. M. Yaghi, *Proc. Natl. Acad. Sci. USA* **2006**, *103*, 10186 – 10191.
[36] S. S. Y. Chui, S. M. F. Lo, J. P. H. Charmant, A. G. Orpen, I. D. Williams, *Science* **1999**, *283*, 1148 – 1150.
[37] B. Zornoza, C. Tellez, J. Coronas, *J. Membr. Sci.* **2011**, *368*, 100 – 109.
[38] B. Zornoza, S. Irusta, C. Tellez, J. Coronas, *Langmuir* **2009**, *25*, 5903 – 5909.
[39] R. A. Munoz, D. Beving, Y. S. Yang, *Ind. Eng. Chem. Res.* **2005**, *44*, 4310 – 4315.
[40] D. W. Fickel, A. M. Shough, D. J. Doren, R. F. Lobo, *Microporous Mesoporous Mater.* **2010**, *129*, 156 – 163.
[41] P. Küsgens, M. Rose, I. Senkovska, H. Frode, A. Henschel, S. Siegle, S. Kaskel, *Microporous Mesoporous Mater.* **2009**, *120*, 325 – 330.
[42] H. J. Yu, Y. M. Cao, G. D. Kang, J. H. Liu, M. Li, Q. Yuan, *J. Membr. Sci.* **2009**, *342*, 6 – 13.
[43] B. Piluharto, V. Suendo, T. Ciptati, C. L. Radiman, *Ionics* **2011**, *17*, 229 – 238.
[44] T. T. Moore, W. J. Koros, *J. Mol. Struct.* **2005**, *739*, 87 – 98.
[45] H. Bux, F. Y. Liang, Y. S. Li, J. Cravillon, M. Wiebcke, J. Caro, *J. Am. Chem. Soc.* **2009**, *131*, 16000 – 16001.
[46] A. Galve, D. Sieffert, E. Vispe, C. Tellez, J. Coronas, C. Staudt, *J. Membr. Sci.* **2011**, *370*, 131 – 140.

Received: July 27, 2011
Published online on September 16, 2011

